

# Fluctuations, Stratification and Stability in a Liquid Fluidized Bed at Low Reynolds Number

P.N. Segrè<sup>1</sup> and J. P. McClymer<sup>2</sup>

<sup>1</sup>Bio-Physics group, NASA Marshall Space Flight Center, Huntsville, AL 35812, USA

<sup>2</sup>Department of Physics, University of Maine, Orono, ME 04469, USA

**Abstract.** The sedimentation dynamics of extremely low polydispersity, non-colloidal, particles are studied in a liquid fluidized bed at low Reynolds number,  $Re \ll 1$ . When fluidized, the system reaches a steady state, defined where the local average volume fraction does not vary in time. In steady state, the velocity fluctuations and the particle concentrations are found to strongly depend on height. Using our results, we test a recently developed stability model [1] for steady state sedimentation. The model describes the data well, and shows that in steady state there is a balancing of particle fluxes due to the fluctuations and the concentration gradient. Some results are also presented for the dependence of the concentration gradient in fluidized beds on particle size; the gradients become smaller as the particles become larger and fewer in number.

## 1. INTRODUCTION

The sedimentation of a collection of monodisperse spheres in liquids is a fundamental problem in physics and is of wide importance in chemical reactors [2]. From numerous experiments [3, 4, 5, 6], computer simulations [7], and theories [8, 9, 10, 11, 12], the following general picture has emerged. On a macroscopic scale, a collection of spheres of size  $D$ , at an average concentration  $\phi_0$ , settle at an average velocity  $v_{sed}(\phi)$ . On a microscopic, or particle scale, however, there are large non-uniformities or fluctuations in both the local concentration  $\sigma_\phi$  and particle velocities  $\sigma_v$ . An examination of the fluctuations [4, 6] show that the particles spontaneously organize themselves into large correlated regions, or blobs, of size  $\xi \gg D$ , as they settle. Significantly, it's been shown that the large scale velocity fluctuations are due to local density fluctuations. Regions where the local concentration is higher than the average fall faster than the average settling rate, while less dense regions fall slower than the average. Extensive experimental work has yielded simple scaling relations for  $\xi$  and  $\sigma_v$  in terms of  $\phi$  and  $a$  [4, 5], yet a consensus on the theoretical origin or understanding of these results is still lacking.

One of the implicit assumptions in many of the experimental and theoretical works in sedimentation is that the properties of the system, including the mean concentration and fluctuation values are uniform throughout the settling process. Recently however, Tee *et al* [13] found that an initially uniform suspension can destabilize and become highly stratified in concentration as the particles settle. In addition, the concentration profiles continued to evolve over the entire settling time. These observations suggest

**Table 1.** Particle and fluidized bed properties.

$D(\mu\text{m})$	$\sigma_D/D$	$\eta$ (cp)	$v_0(\text{mm/s})$	$Re$	$H_{bed}$ (cm)	$\langle\phi_{bed}\rangle$
207	0.015	27	$1.21 \pm 0.03$	0.005	18.5	0.10

that the general assumption of steady state may not always be achieved during sedimentation experiments.

To search for a state of steady state sedimentation, Segré [1] recently conducted experiments in a liquid-solid fluidized bed. In a fluidized bed, liquid is pumped upwards through the column to counteract the force of gravity on the particles. When properly balanced, the particles are perpetually falling, and steady state is ensured. Segré found that all of the properties of the particle dynamics strongly depend upon height in the particle column. A new flux balance model, relating the stratification in concentration to the fluctuations in  $\phi$  and  $v$ , was able to explain the observed stability of the particle column.

In this article, we expand upon this earlier work in two significant ways. First, we test whether particle size polydispersity plays a role in the observed stratification in concentration, by using particles that are much more uniform in size. The beads in this study are among the most monodisperse glass beads commercially available, with a measured size variation of  $\sigma_D/D = 1.5\%$ , as compared to  $\sigma_D/D = 9.5\%$  in the previous work [1]. Our main finding is that a reduction in particle size polydispersity from 9.5 to 1.5% does not significantly change or remove the findings of height dependent properties and concentration stratification. Secondly, we examine how the stratification in concentration observed during steady state sedimentation depends upon particle size and particle number. We conduct a series of experiments on particle columns of identical heights  $H$  and average concentrations  $\phi_0 = 10\%$ , but with particle sizes ranging from  $D = 109$  to  $490$  microns. We find that the degree of stratification changes with particle size and particle number. The fewer the number of particles in the system, the smaller the stratification in concentration.

## 2. EXPERIMENT DESCRIPTION

### 2.1. Particles and Fluids

We use spherical glass beads, of mean diameter  $D = 207\mu\text{m}$ , that have been specially filtered by the manufacturer (Mo-Sci corp.) to be of extremely low polydispersity in size. Fig. [1] shows a micrograph of a collection of the spheres. The particles lay on a flat plate and through a gentle shaking quickly organize into highly ordered forms, indicative of a low size polydispersity. To accurately determine the particle size polydispersity, we measured the variation in settling velocities of 50 individual spheres. The standard deviation of the particle settling rates is indeed extremely low,  $\sigma_v/\langle v \rangle = 3.0\%$ . Using the Stokes formula,  $v_0 \propto \Delta\rho D^2$ , and assuming the particles are all of equal density, the variation in settling rates correspond to a variation in particle size of  $\sigma_D/D = 1.5\%$ .

The glass beads are dispersed in viscous solutions of glycerol and water chosen so that inertial forces during the experiments are negligible. Specifically, the particle Reynolds number is of order  $Re = v_0 a \rho / \eta \approx 5 \times 10^{-3} \ll 1$ . Additionally, particle motions always occur at very high Peclet numbers ( $Pe \approx 10^9$ ), so that Brownian diffusion is negligible. The temperature is at the ambient value  $T = 21^\circ\text{C}$ .

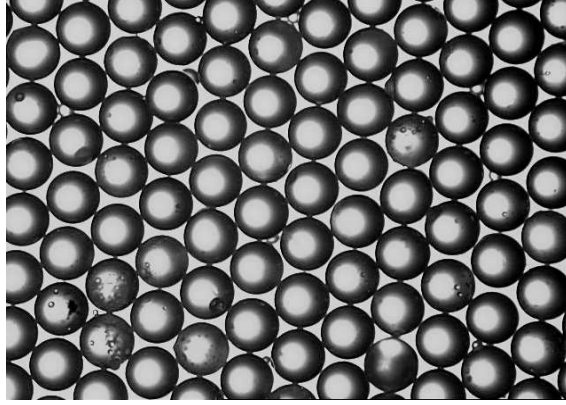


Figure 1. Micrograph of a random sampling of  $D = 207\mu\text{m}$  glass spheres.

## 2.2. Fluidized Bed

The fluidized bed consists of a fluid and particle filled glass cell through which fluid is pumped upwards to counteract the particle settling and *fluidize* the particles. The sample cell is a rectangular glass tube of dimensions  $D \times W \times H = 8 \times 80 \times 305$  mm. The bottom of the cell is glued into a metal base into which the water/glycerol mixture is continuously pumped. The overflow liquid at the top of the cell recirculates back into the pump, forming a closed loop. To enable a uniform flow into the cell, a 2 cm thick nylon mesh is packed with 0.5 mm diameter beads and glued across the entrance to the cell at the bottom.

With the liquid pump off, the spheres fall to the bottom of the cell and form a sediment  $\approx 2.9$  cm tall. When the pump is on, the particles expand upward, filling a region above the bottom up to a height dependent upon the pumped fluid velocity  $v_{pump}$ . We set the pumped fluid velocity to  $v_{pump}/v_0 = 0.727 \pm 0.030$  to expand the particle column expanded to a total height  $H_{bed} \sim 18.5$  cm so that the average volume fraction  $\langle \phi_{bed} \rangle = 0.638 * (2.9/18.5) \sim 0.10$ .

The main feature of a stable fluidized bed is that the average particle velocities in the lab frame are zero; i.e. fluid is pumped upwards at a rate that balances the particle settling rate downwards, and the particles are perpetually sedimenting.

## 2.3. PIV Imaging System: Velocity Flow Maps

Particle velocities are measured using the technique of particle image velocimetry (PIV) [14]. The apparatus consists of a ( $1008 \times 1024$  pixels) CCD camera, a synchronized stroboscope illuminating the cell from behind, and image processing hardware and software from Dantec Instruments. Velocity maps consisting of  $62 \times 62$  vectors are extracted by comparing two closely timed pictures using standard PIV techniques. Each vector is the average velocity of two to four spheres.

Figure 2 shows typical velocity vector maps from a stable fluidized bed, where (a) corresponds to a position near the top and (b) to a position near the middle of the particle column. For scale, we also show the magnitude of the Stokes settling velocity  $v_0$ . Both velocity maps show regions moving both upwards and downwards, but the magnitudes of the velocities are significantly larger near the middle than near the top.

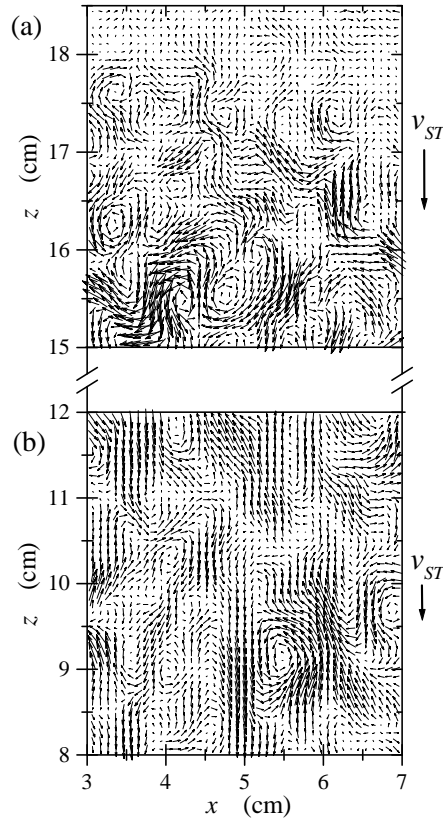


**Figure 2.** Velocity vector maps of a stable fluidized bed at  $\langle \phi_{bed} \rangle = 0.10$ . Figures 1 (a) and (b) correspond to respective positions near to the top and near to the middle of the particle column. The single arrow on the right gives the corresponding scale of the Stokes settling velocity  $v_0$ . Note that the velocity scale in (a) is magnified relative to (b) by a factor of 2 for clarity.

To quantify these observations, we measure the velocity maps and the local volume fractions at different heights along the particle column. We extract from the velocity maps the mean velocities,  $v_x = \langle v_{i,x} \rangle$ , and  $v_z = \langle v_{i,z} \rangle$ , and the root mean square (rms) velocity fluctuations,  $\sigma_v^z = \langle (v_{i,z} - v_z)^2 \rangle^{1/2}$  and  $\sigma_v^x = \langle (v_{i,x} - v_x)^2 \rangle^{1/2}$ , where  $\langle \dots \rangle$  represents an average over  $\sim 50$  vector maps of 3844 vectors each.

#### 2.4. Light Scattering System; Particle Concentrations

Local particle volume fractions are determined using a laser light scattering method that measures the local optical turbidity at various heights in the particle column. To do this, we pass an expanded He-Ne laser beam, of diameter  $\sim 0.5$  cm, through the fluidized bed at a particular height and measure the transmitted laser intensity  $I_T$  using a CCD camera. Results for a typical sample are shown in Fig. 3. Fig. 3(a) shows the measured intensity profiles at different heights in the particle column. It's evident that the transmitted intensity varies with height, with the highest intensity at the top, and the lowest at the bottom. To find the corresponding particle concentrations,

we need a calibration reference for the dependence of the transmitted intensity on particle concentration. To do this, we make several reference fluidized beds of differing average concentration  $\phi_{bed}$  and measure the transmitted intensity patterns at mid-height, shown in Fig. 3(b). Fits of  $I(z)$  and  $I(\phi)$  in Fig. 3(a) and (b) to Gaussian functions yield peak intensity values  $I_{pk}$ . By comparing the measured values of  $I_{pk}(z)$  in our fluidized bed with the reference values of  $I_{pk}(\phi)$  we are able to extract the height dependent concentration  $\phi(z)$  in the fluidized bed.

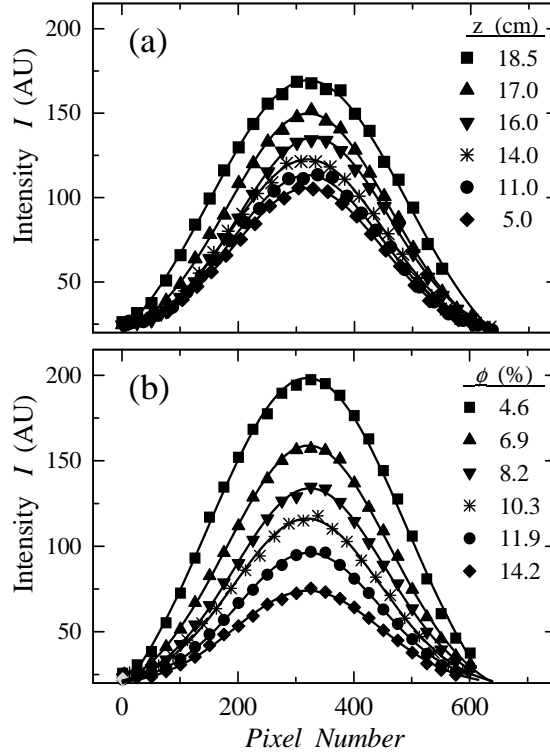


**Figure 3.** Measurement of local particle concentrations. (a) Transmitted laser intensity  $I$  vs. height  $z$  through a fluidized bed at average volume fraction  $\langle\phi\rangle = 0.10$ . (b) Intensity vs.  $\phi$  calibration. Transmitted laser intensities measured at mid-height in fluidized beds of average volume fraction  $0.046 \le \langle\phi\rangle \le 0.142$  as labelled. For clarity, only every 25th point is plotted. The solid lines are fits to Gaussian functions. The height dependent volume fraction  $\phi(z)$  is extracted by comparing the  $I(z)$  curve in (a) with the calibration curve  $I(\phi)$  in (b).

### 3. Results

#### 3.1. Velocity Fields - Fluctuations

Figure 4 displays the values of the average velocities  $v_x$  and  $v_z$ , and the velocity fluctuations  $\sigma_v^x$  and  $\sigma_v^z$  for the stable fluidized bed. Measurements are taken at differing heights from near to the bottom up to the top at a height of  $H_{bed} \sim 18.5$  cm. The average velocities  $v_x \sim 0$  and  $v_z \sim 0$ , indicative of stable fluidization. The velocity

**Table 2.** Measured properties of the fluidized bed described in Table I.  $D$  is the particle diameter and  $N_{tot}$  the total number of particles fluidized.  $v_{pump}/v_o$  is the normalized fluidizing pump velocity upwards.  $v_{top}^{sed}/v_o$  is the initial sedimentation velocity of the top interface, measured just after the fluid pump is turned off.  $\phi_{top}$  is the particle concentration (%) measured just below the top interface. The particle concentrations  $\phi_{top}^{pump}$  and  $\phi_{top}^{sed}$  are calculated from  $v_{pump}/v_o$  and  $v_{sed}/v_o$  using the Richardson-Zaki equation  $v/v_o = (1 - \phi)^{5.5}$ .

$D(\mu m)$	$N_{tot}$	$v_{pump}/v_o$	$v_{top}^{sed}/v_o$	$\phi_{top}$	$\phi_{pump}$	$\phi_{top}^{sed}$
207	$2.7 \cdot 10^6$	$0.727 \pm 0.030$	$0.686 \pm 0.030$	$6.0 \pm 0.3$	$5.6 \pm 0.7$	$6.6 \pm 0.7$

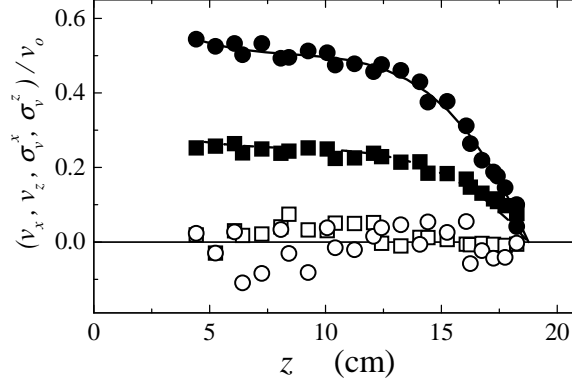


**Figure 4.** Normalized average velocities  $v_x$  (open squares), and  $v_z$  (open circles), and velocity fluctuations  $\sigma_v^x$  (closed squares), and  $\sigma_v^z$  (closed circles), as a function of height  $z$ . The solid lines are polynomial fits to  $\sigma_v^z$ , while the dashed lines are these fits divided by a constant of 2.

fluctuations show a strong height dependence and approach zero magnitude at the top of the particle column. At all heights the level of mixing in the vertical direction is approximately twice that in the horizontal direction, i.e.  $\sigma_v^z \approx 2.0\sigma_v^x$ .

### 3.2. Velocity Fields - Spatial Correlation Lengths

The velocity vector maps, an example of which is shown in Fig. 2, display large regions where the velocity vectors are spatially correlated. To quantify this, we calculate several normalized spatial correlation functions of the vertical velocity  $v_z$ . The first is a longitudinal correlation function, defined as  $C_{ZZ}(z) = \langle v_z(0)v_z(z) \rangle / \langle v_z(0)^2 \rangle$ , and the second is a transverse one, defined as  $C_{ZX}(x) = \langle v_z(0)v_z(x) \rangle / \langle v_z(0)^2 \rangle$ . Here,  $\langle \dots \rangle$  represents an ensemble average over  $\sim 50$  individual vector maps. The correlation functions fit well to the forms  $C_{ZZ}(z) = \exp(-z/\xi_{ZZ})$  and  $C_{ZX}(z) = \exp(-z/\xi_{ZX})$ , allowing us to extract  $\xi_{ZZ}$  and  $\xi_{ZX}$ , the characteristic longitudinal and transverse correlation lengths of the velocity fluctuations. Results for  $\xi_{ZZ}$  and  $\xi_{ZX}$  are shown in Fig. 5. The correlation lengths are not uniform in height, and exhibit a monotonic decrease towards the top part of the column [1].

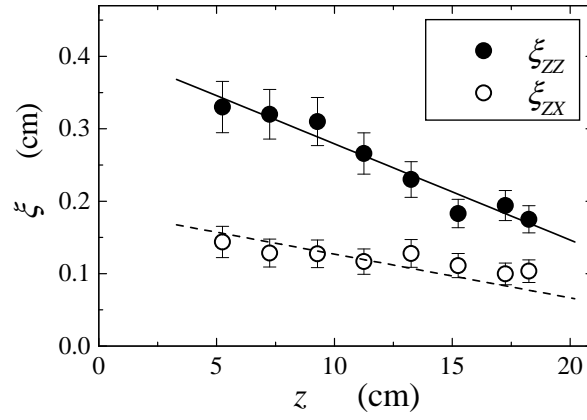


**Figure 5.** (a) Correlation lengths of the velocity fluctuations in the longitudinal,  $\xi_{ZZ}$ , and transverse,  $\xi_{ZX}$ , directions. The lines are linear fits to the data.

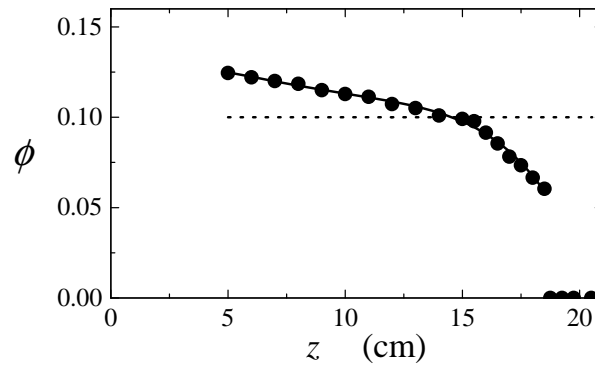


**Figure 6.** Particle volume fraction  $\phi$  as a function of height  $z$ . The dashed line represents the mean particle concentration,  $\phi = 0.10$ .

### 3.3. Concentration Profiles

To examine the concentration profiles, and in particular look for the presence or absence of a vertical density stratification, we use the laser scattering method described in section 2.4 above. This technique allows for highly accurate determinations of the local particle volume fraction  $\phi(z)$  as a function of height  $z$ .

In Fig. 6 we show results for the local particle volume fraction  $\phi(z)$  as a function of height  $z$ . There is a marked stratification in concentration with height; the concentration is significantly greater at the bottom than at the top. Note also the sharp interface at the top, with  $\phi$  dropping from the values  $\phi \sim 0.06$  to  $\phi \sim 0.00$  within  $\sim 0.5$  cm. While most of the concentration variation occurs in the highest portions of the particle column, measurable and significant gradients occur at all heights. For convenience, we refer to the concentration value at the closest measured point to the top interface as  $\phi_{top}$ , and we find  $\phi_{top} = 6.0 \pm 0.3\%$ .

### 3.4. Particle Sedimentation and Fluid Pump Velocities

The stratification in concentration seen in Fig. 6 can help explain the value of the normalized fluid pump velocity  $v_{pump}/v_0$ , listed in Table II. If the particle column were perfectly uniform in concentration at the average value  $\phi_0 = 0.10$ , one would then expect that the upward fluid velocity needed to achieve stable fluidization would be equal and opposite to the sedimentation velocity at volume fraction  $\phi_0$ , i.e.  $v_{pump}/v_0 = -v_{sed}(\phi_0)/v_0$ . To test this, we take advantage of the well known equation for the sedimentation velocity of a collection of spheres at volume fraction  $\phi$ , the Richardson-Zaki (RZ) equation [15],  $v_{sed}(\phi)/v_0 = (1 - \phi)^{5.5}$ . This equation allows us to calculate the sedimentation velocity at average concentration  $\phi = 0.10$ , the value being  $v_{sed}(\phi = 0.10)/v_0 = 0.56$ . As seen in Table II, this value is more than 20% smaller than the measured pump velocity,  $v_{pump}/v_0 = 0.727 \pm 0.030$ . In essence, the velocity of the fluid pumped upwards is *greater* than the average particle sedimentation velocity downwards. The net result, which will be an important component of how fluidized beds stabilize themselves against large fluctuations as discussed in section 4 below, is that the particles are being pushed upwards at all times by this mismatch in sedimentation and pump velocities.

If the fluid pump velocity does not match the calculated sedimentation velocity at  $\phi = 0.10$ , then one can ask at what concentration  $\phi$  does  $v_{pump}$  correspond to? To answer this, we use the value of measured values  $v_{pump}/v_0$  and the RZ equation to calculate  $\phi_{pump} = 1 - (v_{pump}/v_0)^{1/5.5}$ ; we find  $\phi_{pump} = 5.6 \pm 0.7\%$ . Significantly, this value is very similar to the measured concentration at the top of the particle column,  $\phi_{top} \simeq 6.0 \pm 0.3\%$ .

To gain a global perspective of the local settling rates throughout the particle column, we plot in Fig. 7 the calculated sedimentation velocities  $v_{sed}(\phi(z))/v_0 = (1 - \phi(z))^{5.5}$  from the height dependent concentration profiles  $\phi(z)$  shown in Fig. 6. Also indicated by the dashed line is the fluid pump velocity used to achieve stable fluidization. The value of  $v_{pump}/v_0$  closely matches the settling rate at the top of the column, but is significantly greater than  $v_{sed}/v_0$  at all other heights. The net difference between the fluid velocity pumped upwards and the settling velocity downwards is defined as the excess velocity  $v_{ex}/v_0 = [v_{pump} - v_{sed}(z)]/v_0$ .

## 4. Stability Analysis

The results presented above give a rather complete characterization of the concentration profiles and particle velocity dynamics in a stable fluidized bed consisting of extremely low polydispersity spheres ( $\sigma_D/D = 1.5\%$ ). We find that all of the properties measured display marked dependencies on height in the particle column. A fluidized bed can be thought of as a system where the particles are sedimenting *perpetually*. The results for the *rms* velocity fluctuations and the concentration profiles are stable in time and represent the steady state behavior of the system. The finding of steady state behavior has important implications which we can exploit to help understand the concentration and fluctuation profiles observed during fluidization. In section 4.1 below we describe the criterion for fluidized bed stability in terms of a general flux balance relation. In sections 4.1.1, 4.1.2 and 4.2 we evaluate and test this stability criterion using the recently developed model of Segrè [1].

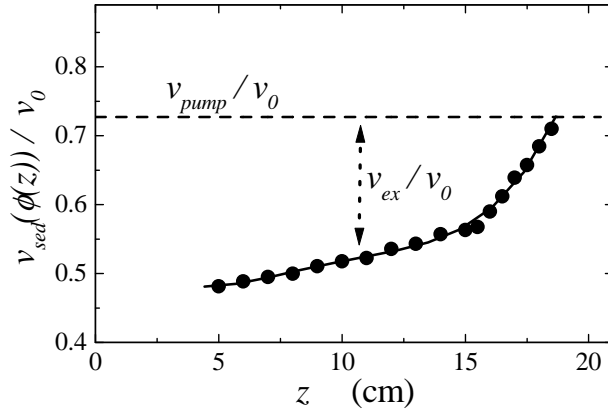


**Figure 7.** Particle sedimentation velocities  $v_{sed}/v_0$ , calculated using the height dependent volume fractions  $\phi(z)$  in Fig. 6 and the Richardson-Zaki equation  $v_{sed}/v_0 = (1 - \phi)^{5.5}$ , as a function of height  $z$ . The dashed line represents the value of the normalized fluid pump velocity,  $v_{pump}/v_0$ , used to stabilize the particle column.

#### 4.1. General Condition for Fluidized Bed Stability.

In steady state the average volume fraction all points in the particle column is constant in time, i.e.  $\partial\phi(z)/\partial t = 0$ . This condition can be written in terms of particle fluxes using the conservation of mass, or continuity, equation  $\partial\phi(z)/\partial t = -\nabla \cdot \mathbf{j}(\mathbf{z}) = 0$  [15], where  $\mathbf{j}(\mathbf{z}) = \phi(z)\mathbf{v}(\mathbf{z})$ , and  $\mathbf{v}(\mathbf{z})$  is a locally coarse grained velocity. To account for the fluctuations in the system, we expand the particle flux to first order,  $\mathbf{j}(\mathbf{z}) = \mathbf{j}_0(\mathbf{z}) + \delta\mathbf{j}(\mathbf{z})$ , and assuming  $\partial j_x/\partial x = \partial j_y/\partial y = 0$ , and  $j(z) = j_z(z)$ , the continuity equation yields a requirement that gradients in the local particle fluxes sum to zero, i.e.

$$\frac{\partial j_0(z)}{\partial z} = -\frac{\partial \delta j(z)}{\partial z}. \quad (1)$$

This stability condition can be integrated to yield

$$j_0(z) = -\int_z^H dz' \left[ \frac{\partial \delta j(z')}{\partial z'} \right], \quad (2)$$

where we have left the fluctuation term in an integral form which will be easier for direct evaluation as described below.

The stability criterion Eq. (2) can be expressed directly in terms of the quantities measured, the particle concentration and velocity fields, by expanding  $\phi(z) \rightarrow \phi_0(z) + \delta\phi(z)$  and  $v(z) \rightarrow v_0(z) + \delta v(z)$ , yielding for the zero'th order particle flux (the LHS of Eq. (2)),

$$j_0(z) = \langle \phi_0(z)v_0(z) \rangle, \quad (3)$$

and for the particle flux due to fluctuations (the RHS of Eq. (2)),

$$\delta j(z) = \langle \phi_0(z)\delta v(z) + \delta\phi(z)v_0(z) + \delta\phi(z)\delta v(z) \rangle \quad (4)$$

where  $\langle \dots \rangle$  represents an ensemble average at each height.

The stability criterion, Eq. (2), expresses the general relationship that must exist for a particle fluidized bed to be stable. To evaluate and test this criterion on our data we need to develop expressions for  $j_0(z)$  and  $\delta j(z)$  in terms of the measured quantities, and we follow closely below the development from Segrè [1].

*4.1.1. Particle Flux Due to the Stratification in Concentration.* The zero'th order particle flux,  $j_0(z) = \langle \phi_0(z)v_0(z) \rangle$  is found from the difference between the mean upward flux due to the pump flow,  $j_{pump}(z) = +\phi(z)v_{pump}$ , and the mean downward flux due to sedimentation,  $j_{sed}(z) = -\phi(z)v_{sed}(z)$ . The net flux is given by the difference

$$j_0(z) = \phi(z)v_{ex}(z) = \phi(z)[v_{pump} - v_{sed}(z)], \quad (5)$$

where we define the excess velocity as  $v_{ex}(z) \equiv v_{pump} - v_{sed}(z)$ . The height dependent sedimentation velocities  $v_{sed}(z)$ , shown in Fig. 7, are calculated from the concentration profiles  $\phi(z)$  and the RZ equation. At the top of the column,  $v_{sed}(z)$  and  $v_{pump}$  are nearly equal, but at all other positions the upward fluid velocity is greater than the downward sedimentation velocities, i.e.  $v_{pump} > v_{sed}(z)$ , resulting in a net particle flux upwards.

*4.1.2. Particle Flux Due to Velocity and Concentration Fluctuations.* The general relation for the particle flux due to fluctuations, Eq. (4), is expressed in terms of the fluctuations in velocity and volume fraction. The first two terms are zero because  $\langle \delta v(z) \rangle = 0$  and  $\langle \delta \phi(z) \rangle = 0$ . The product  $\langle \delta \phi \delta v \rangle$  is non-zero because fluctuations in volume fraction and velocity are correlated [6]. The more concentrated regions move downwards,  $(+\delta \phi)(-\delta v)$ , and the less concentrated regions move upwards,  $(-\delta \phi)(+\delta v)$ , so that  $\delta j(z) < 0$  and fluctuations result in a net particle flux *downwards*. To estimate  $\delta \phi$ , we use a simple model based upon random statistics [2]. Fluctuations occur in regions of linear size  $\xi$ , and contain on average  $N_\xi = \phi \xi^3 / a^3$  particles, assuming that the particles are randomly distributed. The rms fluctuations are determined as  $\sigma_{N_\xi} = \sqrt{N_\xi S(\phi)}$ , where  $S(\phi)$  accounts for excluded volume effects and is calculated from the Carnahan-Starling equation for hard spheres [15]. The rms fluctuations in volume fraction are then  $\sigma_\phi = \sigma_{N_\xi} (a/\xi)^3 = \sqrt{\phi S(\phi) a^3 / \xi^3}$ .

Approximating the values of  $\delta \phi \rightarrow \sigma_\phi$  and  $\delta v \rightarrow \sigma_v^z$ , and replacing the derivative term as  $\partial/\partial z \rightarrow C_\xi/\xi$ , where  $C_\xi$  is an adjustable constant expected to be of order unity, the flux due to fluctuations is

$$\partial[\delta j(z)]/\partial z \simeq -C_\xi \sigma_\phi \sigma_v / \xi, \quad (6)$$

which can be written out in terms of the measured quantities using the expression for  $\sigma_\phi$  as

$$\partial[\delta j(z)]/\partial z = -C_\xi \sigma_v^z(z) \sqrt{S(\phi) \phi(z) a^3 / \xi(z)^5}. \quad (7)$$

The negative values of  $\delta j(z)$  indicate the coupling of velocity and concentration fluctuations results in a net flux of particles downwards. The particle flux due to fluctuations, the RHS of Eq. (2), is then

$$\delta j(z) = -C_\xi \int_z^H \sigma_v^z(z') \sqrt{\frac{S(\phi) \phi(z') a^3}{\xi(z')^5}} dz' . \quad (8)$$

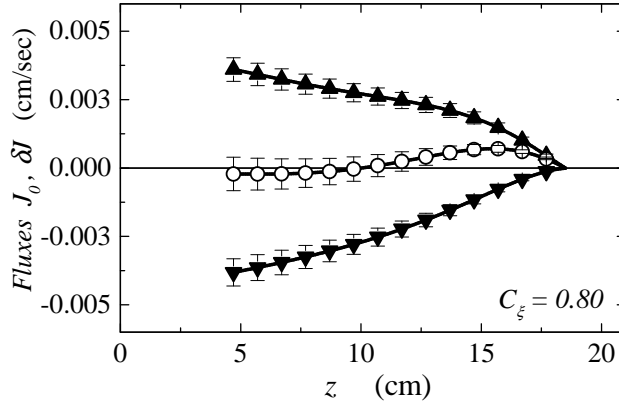


**Figure 8.** Stability test: Particle fluxes  $j_0(z)$  (up triangle), from Eq. (5), and  $\delta j(z)$  (down triangle), from Eq. (8), and their sum  $j_0(z) + \delta j(z)$  (o) as a function of height  $z$  in stable fluidized bed. With the constant  $c_\xi = 0.80$  the particle fluxes sum to near zero at all heights, indicative of a stable, steady state particle column.

#### 4.2. Test of Criterion for Fluidized Bed Stability

We now explicitly test the stability condition, Eq. (2), using the expressions for  $j_0(z)$  and  $\delta j(z)$  in Eqs. (5) and (8). All of the variables needed to evaluate Eqs. (5) and (8), with the exception of  $v_{sed}(z)$ , were directly measured. The sedimentation velocities  $v_{sed}(z)$  were calculated from our data for  $\phi(z)$  using the RZ equation [15]. Polynomial fits to our data for  $\phi(z)$ ,  $\xi(z)$  and  $\sigma_v^z(z)$  were used in the evaluation.

The results for the particle fluxes due to the concentration stratification,  $j_0(z)$ , the velocity and concentration fluctuations,  $\delta j(z)$ , and their sum,  $j_0(z) + \delta j(z)$ , are shown in Fig. 8. The values for  $j_0(z)$  indicate near zero net flux at the top of the bed, due to the matching of the pumped fluid and particle sedimentation velocities, and *positive* and increasing fluxes towards the lower part of the bed where the pumped fluid velocities are greater than the local sedimentation rates. At the top of the column  $\delta j(z)$  also vanishes due to the vanishing of the velocity fluctuations, while *negative* and increasing fluxes are found towards the lower part of the bed where the fluctuations in  $\sigma_v^z(z)$  and  $\sigma_\phi(z)$  become larger.

Strikingly, the net particle flux, obtained from summing the integrals of the two flux gradient terms, i.e.  $j_0(z)$  and  $\delta j(z)$  together, is near zero over the entire height of the column. These results show that the particle column is stable because the particle flux downward due to fluctuations is nearly equal and opposite to the flux upwards due to the stratification in  $\phi v_{ex}$ . The equality of the flux gradients leads to the stability relation, expressed in derivative form,

$$\frac{\partial[\phi(z)v_{ex}(z)]}{\partial z} = -C_\xi \sigma_v^z(z) \sqrt{\frac{S(\phi)\phi(z)a^3}{\xi(z)^5}}, \quad (9)$$

which shows that the magnitudes of the fluctuations are related to the degree of stratification.

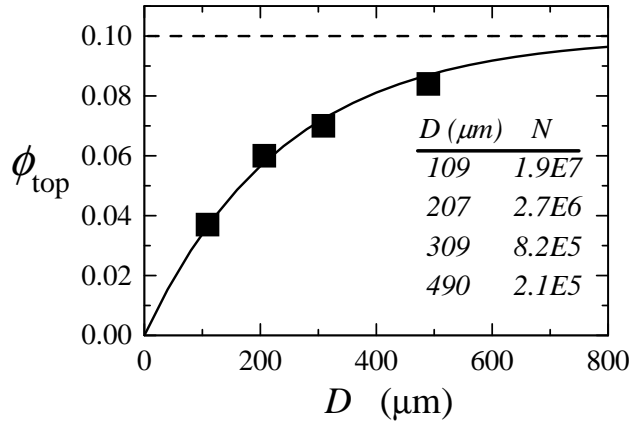


**Figure 9.** Measured volume fraction at the top of the particle columns,  $\phi_{top}$ , as a function of particle diameter  $D$ . The solid line is a guide to the eye. The dashed line represents the mean concentration in all the beds,  $\phi_0 = 0.10$ , and  $N$  is the total number of particles in each fluidized bed.

#### 4.3. Fluidized Beds with Varying Particle Sizes

The results above show that a strong stratification in concentration is present during fluidization; the concentration at the top of the particle column is significantly lower than the mean. How does this stratification vary with particle size or the number of particles in the system? To answer this, we examine a series of 4 fluidized beds with identical mean concentrations,  $\phi_0 = 0.10$ , identical particle column heights,  $H \approx 18.5$  cm, but differing particle sizes, with  $D = 109, 207, 309$ , and  $490 \mu m$ . While a full accounting of these experiments is in preparation [16], we show in Fig. 9 measured values of the volume fraction just below the top interface,  $\phi_{top}$ . The degree of stratification changes with particle size. For the largest particles,  $D = 490 \mu m$ , the difference of the top from the mean ( $\phi = 0.10$ ) is only  $\Delta\phi = (0.10 - \phi_{top}) \sim 0.016$ . With decreasing particle size this value increases significantly, equaling  $\Delta\phi \sim 0.063$  for the smallest particles. In terms of the total number of particles  $N$  fluidized, the system becomes more uniform as  $N$  decreases.

## 5. Conclusions

The sedimentation dynamics of non-colloidal spheres are studied in a liquid fluidized bed at low Reynolds number. The spheres are of much higher uniformity in size than those used in prior studies [1]. During fluidization, the system reaches a steady state, defined where the local average volume fraction does not vary in time. In steady state, the velocity fluctuations and the particle concentrations are found to strongly depend on height. Using our results, we test a recently developed stability model [1] for steady state sedimentation. The model describes our data well, and shows that in steady state there is a balancing of particle fluxes due to the fluctuations and the concentration gradient. Some results are also presented for the dependence of the concentration gradient in fluidized beds on particle size; the gradients become smaller as the particles become larger and fewer in number. The large question that remains as yet unanswered is what controls the degree of particle stratification or the fluctuation

magnitudes. The stability model connects together these two quantities, but cannot *a priori* predict either of their values in the absence of knowledge of the other.

We thank Shang Tee and Tony Ladd for discussions, in particular for stressing the importance of using nearly monodisperse beads.

\*Corresponding author, phil.n.segre@nasa.gov

## References

- [1] Segrè P N 2002 *Phys. Rev. Lett.* **89** 254503.
- [2] Hinch E J, in *Disorder in Mixing*, edited by Guyon E *et al.*, Kluwer Academic, Dordrecht, 1988, p. 153.
- [3] Nicolai H and Guazzelli E 1995 *Phys. Fluids* **7** 3; Nicolai H, Herzhaft B, Hinch E J, Oger L, and Guazzelli E, *Phys. Fluids* **7** 12.
- [4] Segrè P N, Herbolzheimer E and Chaikin P M 1997 *Phys. Rev. Lett.* **79** 2574.
- [5] Segrè P N, Liu F, Umbanhower P and Weitz D A 2001 *Nature* **409** 594.
- [6] Lei X, Ackerson B J, and Tong P 2001 *Phys. Rev. Lett.* **86** 3300.
- [7] Ladd A J C 1996 *Phys. Rev. Lett.* **76** 1392; 2002 *Phys. Rev. Lett.* **88** 48301.
- [8] Caffisch R E and Luke J H C 1985 *Phys. Fluids* **28** 259.
- [9] Koch D L and Shaqfeh E S G 1991 *J. Fluid Mech.* **224** 275.
- [10] Levine A, Ramaswamy S, Frey E and Bruinsma R 1998 *Phys. Rev. Lett.* **81** 5944.
- [11] Tong P and Ackerson B J 1998 *Phys. Rev. E* **58** XXX.
- [12] Brenner M P 1999 *Phys. Fluids* **11** 754.
- [13] Tee S Y, Mucha P J, Cipelletti L, Manley S, Brenner M P, Segrè P N and Weitz D A 2002 *Phys. Rev. Lett.* **89** 54501.
- [14] Adrian R J 1991 *Annu. Rev. Fluid Mech.* **23** 261.
- [15] Russel W B, Saville D A and Schowalter W R 1989 *Colloidal Dispersions* (Cambridge Univ. Press, Cambridge).
- [16] Segrè P N and McClymer J P 2004, in preparation.